


# $TiS_2$-graphene heterostructures enabling polysulfide anchoring and fast electrocatalyst for lithium-sulfur batteries: A first-principles calculation

Wenyang Zhao(赵文阳), Li-Chun Xu(徐利春), Yuhong Guo(郭宇宏), Zhi Yang(杨致), Ruiping Liu(刘瑞萍), and Xiuyan Li(李秀燕)

**Citation:**Chin. Phys. B, 2022, 31 (**4**): 047101. DOI: 10.1088/1674-1056/ac3227
Journal homepage: http://cpb.iphy.ac.cn; http://iopscience.iop.org/cpb

**What follows is a list of articles you may be interested in**

---

## Accurate $GW_0$ band gaps and their phonon-induced renormalization in solids

Tong Shen(申彤), Xiao-Wei Zhang(张小伟), Min-Ye Zhang(张旻烨), Hong Jiang(蒋鸿), and Xin-Zheng Li(李新征)
Chin. Phys. B, 2021, 30 (**11**): 117101. DOI: 10.1088/1674-1056/ac0041

## Anisotropic thermoelectric transport properties in polycrystalline $SnSe_2$

Caiyun Li(李彩云), Wenke He(何文科), Dongyang Wang(王东洋), and Li-Dong Zhao(赵立东)
Chin. Phys. B, 2021, 30 (**6**): 067101. DOI: 10.1088/1674-1056/abeee1

## Vanadium based $XVO_3$ ($X$=Na, K, Rb) as promising thermoelectric materials: First-principle DFT calculations

N A Noor, Nosheen Mushahid, Aslam Khan, Nessrin A. Kattan, Asif Mahmood, Shahid M. Ramay
Chin. Phys. B, 2020, 29 (**9**): 097101. DOI: 10.1088/1674-1056/ab99ad

## Electronic structure from equivalent differential equations of Hartree-Fock equations

Hai Lin(林海)
Chin. Phys. B, 2019, 28 (**8**): 087101. DOI: 10.1088/1674-1056/28/8/087101

## Anisotropic elastic properties and ideal uniaxial compressive strength of $TiB_2$ from first principles calculations

Min Sun(孙敏), Chong-Yu Wang(王崇愚), Ji-Ping Liu(刘吉平)
Chin. Phys. B, 2018, 27 (**7**): 077103. DOI: 10.1088/1674-1056/27/7/077103

---

# $TiS_2$–graphene heterostructures enabling polysulfide anchoring and fast electrocatalyst for lithium-sulfur batteries: A first-principles calculation

Wenyang Zhao(赵文阳), Li-Chun Xu(徐利春)†, Yuhong Guo(郭宇宏), Zhi Yang(杨致), Ruiping Liu(刘瑞萍), and Xiuyan Li(李秀燕)

*College of Physics and Optoelectronics, Taiyuan University of Technology, Taiyuan* 030024, *China*

(Received 31 July 2021; revised manuscript received 17 September 2021; accepted manuscript online 22 October 2021)

Lithium-sulfur batteries have attracted attention because of their high energy density. However, the "shuttle effect" caused by the dissolving of polysulfide in the electrolyte has greatly hindered the widespread commercial use of lithium-sulfur batteries. In this paper, a novel two-dimensional $TiS_2$/graphene heterostructure is theoretically designed as the anchoring material for lithium-sulfur batteries to suppress the shuttle effect. This heterostructure formed by the stacking of graphene and $TiS_2$ monolayer is the van der Waals type, which retains the intrinsic metallic electronic structure of graphene and $TiS_2$ monolayer. Graphene improves the electronic conductivity of the sulfur cathode, and the transferred electrons from graphene enhance the polarity of the $TiS_2$ monolayer. Simulations of the polysulfide adsorption show that the $TiS_2$/graphene heterostructure can maintain good metallic properties and the appropriate adsorption energies of 0.98–3.72 eV, which can effectively anchor polysulfides. Charge transfer analysis suggests that further enhancement of polarity is beneficial to reduce the high proportion of van der Waals (vdW) force in the adsorption energy, thereby further enhancing the anchoring ability. Low $Li_2S$ decomposition barrier and Li-ion migration barrier imply that the heterostructure has the ability to catalyze fast electrochemical kinetic processes. Therefore, $TiS_2$/graphene heterostructure could be an important candidate for ideal anchoring materials of lithium-sulfur batteries.

**Keywords:** lithium-sulfur batteries, $TiS_2$/graphene heterostructure, anchoring material, shuttle effect

**PACS:** 71.15.–m, 71.20.–b, 71.15.Mb, 31.15.A– **DOI:** 10.1088/1674-1056/ac3227

## 1. Introduction

With the rapid development of electronics and electric vehicles, there is an increasing demand for rechargeable batteries with higher energy density and longer cycle life. Lithium-ion/sodium-ion batteries have been successfully used in portable electronic devices and electric vehicles.[1–4] However, the lower energy density limits its large-scale application in the future commercial markets. In recent years, lithium-sulfur batteries have attracted extensive attention from researchers because of their high energy density (2600 Wh/kg), high theoretical capacity (1675 mAh/g), low cost, and non-toxic nature.[5–8] However, the development of lithium-sulfur batteries is hampered by their own inherent limitations. First of all, the poor electronic conductivity of sulfur and its discharge products leads to the larger internal resistance of the battery, which affects the performance of the battery rate. Secondly, there is the "shuttle effect" in lithium-sulfur batteries. During the discharge process, lithium polysulfide is easily dissolved in the electrolyte and diffuses to the anode under the action of concentration gradient, which leads to partial sulfur irreversible deactivation and reduces the utilization rate of lithium, and seriously affects the cycle stability and coulomb efficiency of lithium-sulfur batteries. Thirdly, the volume of sulfur changes dramatically (up to 80%) during charge and discharge, which may lead to the collapse of the internal structure, and thus affects the cycle performance of the battery.

In order to solve the above problems, researchers have made many attempts, especially at improving the shuttle effect of polysulfide. One solution is to combine sulfur with the host material to build the composite cathode. At present, two-dimensional (2D) materials are undoubtedly the important candidates for the cathode host materials of lithium-sulfur batteries. For example, graphene,[9–11] Mxene,[12,13] transition metal sulfide,[14] and other two-dimensional materials have strong mechanical stability, flexibility, and very large specific surface area, which are suitable as cathode host materials for lithium-sulfur batteries. Among all these cathode host materials, graphene is an ideal material for hosting sulfur because of its high mechanical strength and electrical conductivity. It can play a very important role in volume expansion suppression, multi-sulfur intermediate conversion, and electron transport in the discharge process.[15,16] However, because of the non-polar feature of graphene, it cannot continue to play an anchoring role in multiple cycles. Considering the great potential of reduced graphene oxide (RGO) in the direction of flexibility and the ability to enhance polarity, exploring the application of RGO in lithium-sulfur batteries may be an important development direction. However, how to overcome the problems of poor mechanical properties and electrical conduc-

†Corresponding author. E-mail: xulichun@tyut.edu.cn

© 2022 Chinese Physical Society and IOP Publishing Ltd 

tivity for RGO still needs a lot of work. The current approach is to change the polarity of graphene by doping,[17] adsorbing groups,[18] or constructing van der Waals polarity heterostructure. The first two methods are more difficult to control experimentally, and the method based on heterostructure is more maneuverable. A $VS_2$/graphene composite structure has been constructed as a sulfur material host by the Zhang group.[19] Benefit from the strong electrical conductivity of graphene and the polarity of $VS_2$, the shuttle and volume expansion of polysulfides are effectively inhibited by structural reinforcement and chemical anchoring. The capacity of 532 mAh/g can still be maintained after 300 cycles at high magnification. Mantiram *et al.* also attempted to use $MoS_2$/graphene heterostructure as a lithium-sulfur anode host material, maintaining a capacity of nearly 600 mAh/g after 500 cycles at 1 C rate.[20] Currently, there are few reports on the theoretical research on the use of heterostructure as an anchoring material for lithium-sulfur batteries.

In order to clarify the microscopic mechanism of the heterostructure enhanced lithium-sulfur battery, we designed a novel 2D $TiS_2$/graphene heterostructure as an anchoring material for lithium-sulfur batteries in this work. Its structural and electronic properties, the anchorage of polysulfides, and the diffusion barrier of Li-ion were analyzed theoretically by density functional theory calculation. The calculation results show that $TiS_2$/graphene heterostructure not only has excellent electrical conductivity but also shows strong anchoring of polysulfide and low Li-ion diffusion barrier, which proves that $TiS_2$/graphene heterostructure is an ideal anchoring material for lithium-sulfur batteries. Our simulation provides theoretical guidance for further preparation of advanced electrode materials for lithium-sulfur batteries.

## 2. Computational method

All first-principles calculations in this paper were carried out by using the density functional theory (DFT) in the Vienna *ab initio* simulation package (VASP).[21] Perdew–Burke–Ernzerhof (PBE) functional of the generalized gradient approximation (GGA) was employed to treat the electronic exchange-correlation energy.[22] The projector augmented wave (PAW) method was used to describe the electron–ion interactions,[23] and the cut-off energy of the plane wave was set to be 500 eV. The Monkhorst–Pack (MP) method of $k$-mesh sampling was adopted for integration over the first Brillouin zone. In the process of optimizing the 2D structure and calculating the molecular adsorption, a $3\times3\times1$ $k$-mesh sampling was applied. The $k$-mesh sampling was increased to $10\times10\times1$ when calculating the electronic properties. Both cut-off energy and $k$-point mesh were carefully tested and ensured that the convergence error is within 1 meV. The energy convergence criterion was all set to be $10^{-5}$ eV, and the force was selected as 0.01 eV/Å. In order to avoid the interaction between layers caused by periodic boundary conditions, we set the vacuum layer in the $z$-direction at 13.9 Å. Considering the influence of long-range vdW interaction, Grimme's DFT-D3 method was used to describe it.[24,25] The spin-polarized calculations were implemented, and the results showed that the effect of spin polarization on the results could be ignored. The decomposition barrier of $Li_2S$ and the migration barrier of Li-ion on the surface of the heterostructure were simulated by the climbing-image nudged elastic band (CI-NEB) method.[26,27]

In order to study the anchored properties of the $TiS_2$/graphene heterostructure, a large number of different adsorption structures were constructed. By comparing the adsorption energies, the adsorption structure with the lowest energy was selected as the best adsorption configuration. The adsorption energy was calculated by

$$E_{\text{ads}} = E_{\text{system}} - \left(E_{S_8/Li_2S_n} + E_{\text{substrate}}\right), \tag{1}$$

where $E_{\text{system}}$, $E_{S_8/Li_2S_n}$ and $E_{\text{substrate}}$ refer to the energies of the adsorption system, isolated $S_8/Li_2S_n$ molecule and substrate, respectively. When calculating the binding energy of long-chain lithium polysulfides with two solvent molecules, an adsorption model of Li–O bond bonding between an O atom in the solvent molecule and a Li atom in lithium polysulfides was used.[28,29] In addition, to further investigate the interaction between polysulfides and $TiS_2$/graphene heterostructure, the charge density difference diagrams (CDD) were drawn and the amount of charge transfer between polysulfides and substrate was quantitatively calculated by Bader charge analysis.[30] The charge density difference ($\Delta\rho$) is defined as

$$\Delta\rho = \rho_{Li_2S_n+\text{substrate}} - \left(\rho_{Li_2S_n} + \rho_{\text{substrate}}\right), \tag{2}$$

where $\rho_{Li_2S_n+\text{substrate}}$, $\rho_{Li_2S_n}$ and $\rho_{\text{substrate}}$ indicate the charge density of the absorption system, isolated $Li_2S_n$ molecule and substrate, respectively.

## 3. Results and discussion

Van der Waals heterostructures are usually formed between two-dimensional materials. The optimal lattice constants of the used $TiS_2$ monolayer and graphene are 3.42 Å and 2.46 Å. Since the constituent monolayers have different lattice constants, it is necessary to minimize strain when constructing an atomic model of the heterostructure. The construction method is as follows. We denote the primitive-cell basis vectors of the constituent monolayer $i$ as $\{\boldsymbol{a}_i, \boldsymbol{b}_i\}$, then the supercell basis vector can be expressed as $n_i\boldsymbol{a}_i + m_i\boldsymbol{b}_i$. To minimize the interface strain of the constructing heterostructure, the magnitude of the supercell basis vectors in monolayers $i$ and $j$ should approximately match: $|n_i\boldsymbol{a}_i + m_i\boldsymbol{b}_i| \approx |n_j\boldsymbol{a}_j + m_j\boldsymbol{b}_j|$. In practice, we searched all sets of integers within 10, then chose the smallest supercell for which the strain is less than

0.5%. The resulting heterostructure was finally constructed with a $\sqrt{13} \times \sqrt{13}$ $TiS_2$ supercell ($n = 1$, $m = 4$) and a $5 \times 5$ graphene supercell ($n = 0$, $m = 5$), and the lattice constant of the heterostructure used the average of the lattice constants of the two supercells. The total number of atoms corresponding to this heterostructure reached 89, and the mean absolute stress of the interface was only 0.08%. It satisfies the matching requirements of a van der Waals heterostructure.[31,32] After atomic-position optimization and layer-shift confirmation, the layer spacing between the $TiS_2$ monolayer and graphene is confirmed as 3.35 Å, which is a typical layer spacing (3–4 Å) for the van der Waals heterostructure.

To verify the stability of the $TiS_2$/graphene heterostructure, the phonon spectrum of monolayer $TiS_2$ has been calculated and found that there is no imaginary frequency in the phonon spectrum, which implies that monolayer $TiS_2$ is a dynamically stable structure. The *ab initio* molecular dynamics (AIMD) simulations were also carried out at three temperatures of 300 K, 500 K and 1000 K, and it was found that the structure did not undergo a phase change after 10 ps of time evolvement. Therefore, the $TiS_2$/graphene heterostructure is theoretically a stable structure.

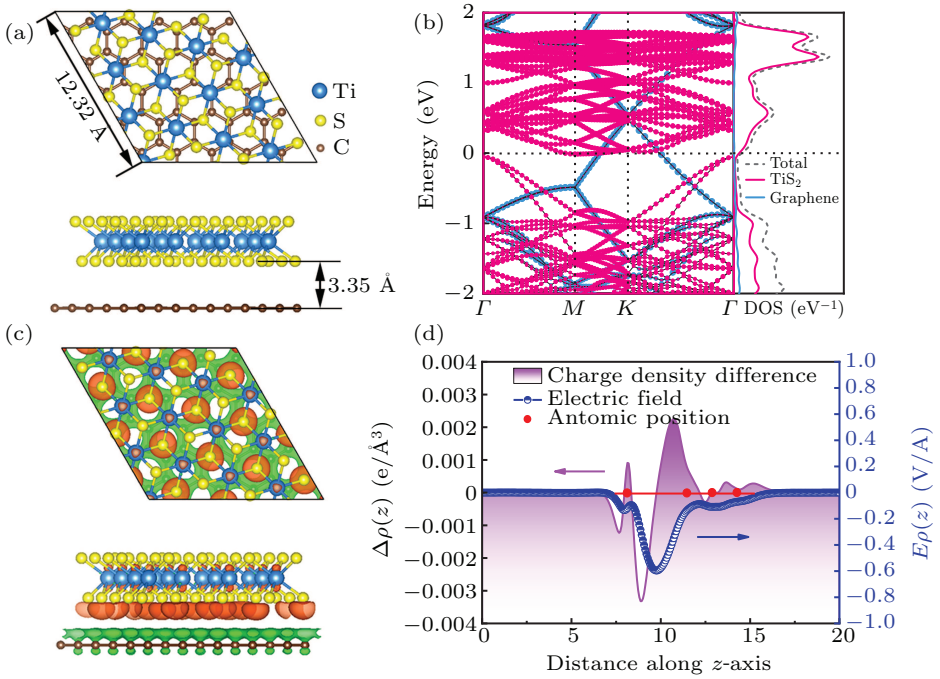



**Fig. 1.** (a) The top and side views of the structurally optimized $TiS_2$/graphene heterostructure. (b) Electronic band structure and density of states (DOS) of $TiS_2$/graphene heterostructure. (c) Charge density difference (CDD) between $TiS_2$ monolayer and graphene. The isosurface level is set to 0.0004 e·Å$^{-3}$. The orange and green regions represent electron accumulation and depletion, respectively. (d) Planar average charge density difference and the response electric field along the $z$-direction between $TiS_2$ monolayer and graphene.

The electronic conductivity is an important factor affecting the rate performance of the electrode materials for lithium-sulfur batteries. To investigate the electronic properties of $TiS_2$/graphene heterostructure, we calculated its electronic band structure and density of state (DOS). As shown in Fig. 1(b), the energy bands cross through the Fermi level, indicating that the heterostructure has a good metallic property. The orbital composition analysis shows that the formation of the heterostructure does not significantly change the electronic structures of the $TiS_2$ monolayer and graphene, which ensures that the graphene with excellent electronic conductivity can improve the electronic conductivity of the sulfur cathode. Moreover, the Dirac point of graphene shifts above the Fermi level, leading to the formation of p-type doped graphene, which implies that the charge of graphene is transferred to the $TiS_2$ monolayer. To visually display the charge redistribution between layers, the charge density difference (CDD) between the $TiS_2$ monolayer and graphene was calculated. As can be seen from Fig. 1(c), charge transfer exists between graphene and the $TiS_2$ monolayer, and charge (0.43 e) is transferred from the C atoms of graphene to the inner S atoms and Ti atoms of the $TiS_2$ monolayer. The main charge redistribution occurs between the layers, and this type of interlayer dipole is conducive to the stability of the heterostructure. The planar charge density difference (PCDD) and the associated response electric field along the $z$-direction in Fig. 1(d) give a more quantitative result. The positive value of $\Delta\rho$ represents the accumulation of charge, while the negative value represents the dissipation of charge.[33,34] By using the Poisson equation $\nabla^2 V(z) = -\Delta\rho/\varepsilon_0$, the integration of the charge density difference, $\Delta\rho$, along the direction perpendicular to the layers, results in a response electric field (blue line in Fig. 1(d)). The PCDD diagram also shows that charge transfer mainly occurs at the interface between layers. A large response electric field

appears at the interface, corresponding to the charge depletion at the graphene surface and the charge accumulation at the $TiS_2$ surface, which leads to the interlayer polarization. The redistribution of charge in the $TiS_2$ layer also corresponds to a small response electric field, leading to the intralayer polarization. Therefore, the charge transfer enhances the polarity of the $TiS_2$ material, and the outer surface of the $TiS_2$ monolayer has a small amount of charge accumulation, which benefits the enhance of the anchoring effect on polysulfides.

Before studying the adsorption of polysulfides on the surface of the heterostructure, the structures of polysulfides have been carefully optimized. In lithium-sulfur batteries, the cathode sulfur usually exists as the most stable allotrope, orthogonal $\alpha$-$S_8$.[35] During the discharge, the lithium in the anode is dissolved in the electrolyte and transferred from the anode to the cathode, where it reacts with the sulfur in the cathode to form a series of lithium polysulfides ($Li_2S_n$, $n = 8$, 6, 4, 2 and 1). The most stable structures of polysulfides molecular after geometric optimization are shown in Fig. 2. The results show that all atoms in the polysulfides are neither in a straight line nor in a plane. The polysulfides are more inclined to three-dimensional (3D) structures rather than two-dimensional (2D) chains, which is also consistent with the results of previous studies.[36,37] In addition, with the decrease of the number of sulfur atoms in the lithium polysulfides, the length of the Li–S bond becomes shorter and the bond cooperation increases gradually. Therefore, compared with the short-chain lithium polysulfides ($Li_2S_n$, $n = 1$, 2), the long-chain lithium polysulfides ($Li_2S_n$, $n = 4$, 6, 8) tend to dissolve in the electrolyte and ionize into lithium cations and polysulfide anions, resulting in the shuttle effect.

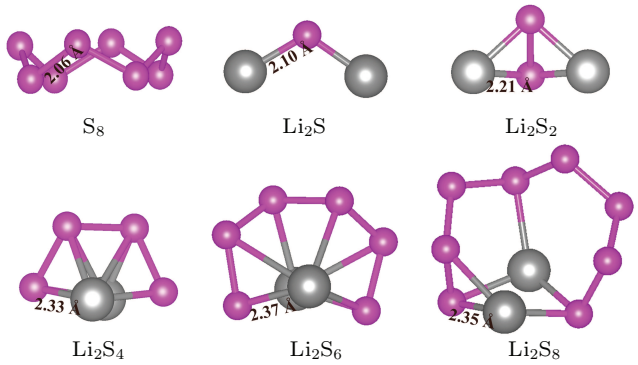



**Fig. 2.** The optimized structures of polysulfides.

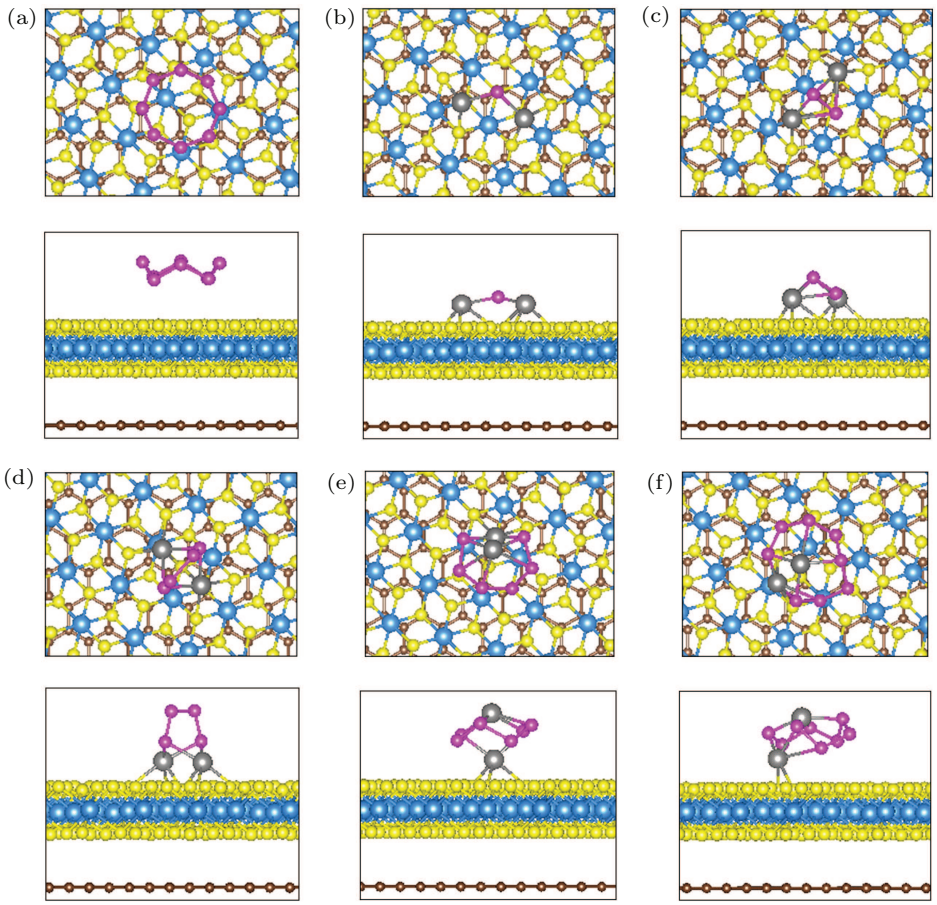



**Fig. 3.** The top and side views of the most stable adsorption structures of (a) $S_8$, (b) $Li_2S$, (c) $Li_2S_2$, (d) $Li_2S_4$, (e) $Li_2S_6$, (f) $Li_2S_8$ molecules adsorbed on the surface of $TiS_2$/graphene heterostructure. The purple and yellow atoms represent the sulfur atoms in the polysulfides and substrate, respectively.

The ideal anchoring materials for lithium-sulfur batteries should have reinforcing interactions with polysulfide intermediates to ensure their cyclic stability. Therefore, to evaluate the anchoring effect of polysulfides on the surface of the heterostructure, we designed and optimized the adsorption structures of polysulfides with different orientations at different adsorption sites on the surface of the heterostructure, and then calculated the adsorption energy of these structures. The adsorption configurations with the lowest adsorption energy are shown in Fig. 3. The sulfur-atom ring of the $S_8$ molecule is parallel to the surface of the $TiS_2$/graphene heterostructure, without the formation of the chemical bond between them. The minimum distance between the $TiS_2$ monolayer and $S_8$ is about 3.27 Å, which is much larger than the bond length (< 2.7 Å) of a typical chemical bond. During the discharge process, lithium ions are inserted into the sulfur cathode to form a series of lithium polysulfides. For long-chain molecules $Li_2S_6$ and $Li_2S_8$, only one Li atom bonds with the surface sulfur of the heterostructure, the other Li atom is far away from the surface of the heterostructure, and the S atoms of long-chain molecules form a ring, which is approximately parallel to the surface of the heterostructure. The larger coordination number of lithium limits its continued bonding with more sulfur. Therefore, both lithium atoms in the short-chain $Li_2S_n$ ($n = 1, 2, 4$) molecules tend to bond with the sulfur on the surface of the heterostructure, and the sulfur-atom ring of $Li_2S_4$ are perpendicular to the surface of the heterostructure. By observing all the adsorption structures in Fig. 3, it could be found that all the polysulfides adsorbed on the surface of the heterostructure have no obvious deformation and decomposition. Therefore, when polysulfide molecules are formed, they can be effectively anchored on the $TiS_2$ monolayer surface without harmful side reactions.

It is well known that the shuttle effect of long-chain lithium polysulfides ($Li_2S_n$, $n = 4, 6, 8$) dissolved in electrolyte seriously affects the cycle stability and coulomb efficiency of lithium-sulfur batteries. Therefore, to study whether the $TiS_2$/graphene heterostructure can effectively anchor lithium polysulfides, we compared the adsorption energies of long-chain lithium polysulfides ($Li_2S_n$, $n = 4, 6, 8$) on the surface of the heterostructure and their binding energy with two typical electrolyte solvent molecules (DOL, DME). As shown in Fig. 4(a), the $TiS_2$/graphene heterostructure can maintain an appropriate adsorption energy higher than 1.5 eV for long-chain lithium polysulfides. More importantly, the adsorption energies of long-chain lithium polysulfides with the $TiS_2$/graphene heterostructure are significantly greater than their respective binding energy with solvent molecules, which indicates that $TiS_2$/graphene heterostructure, as the anchoring material of lithium-sulfur batteries, can prevent lithium polysulfides from dissolving in the electrolyte, thus avoiding the loss of active substances due to the shuttle effect. To make the calculations of the adsorption energies more reliable, the GGA+$U$ method has been adopted, and the $U$ value of Ti 3d orbital is 2.1. As shown in Fig. 4(a), the adsorption energies calculated by the GGA+$U$ method are lower than those calculated by the GGA method. This is mainly because the GGA+$U$ method enhances the locality of Ti-d orbitals and the repulsive force between the electrons, and then decreases the adsorption force between the polysulfide molecules and the heterostructure. Nevertheless, the GGA+$U$ modified adsorption energies are still much higher than the binding energy with two typical electrolyte solvent molecules (DOL, DME). Therefore, it is possible to confirm the high-efficiency anchoring effect of the heterostructure based on different methods.

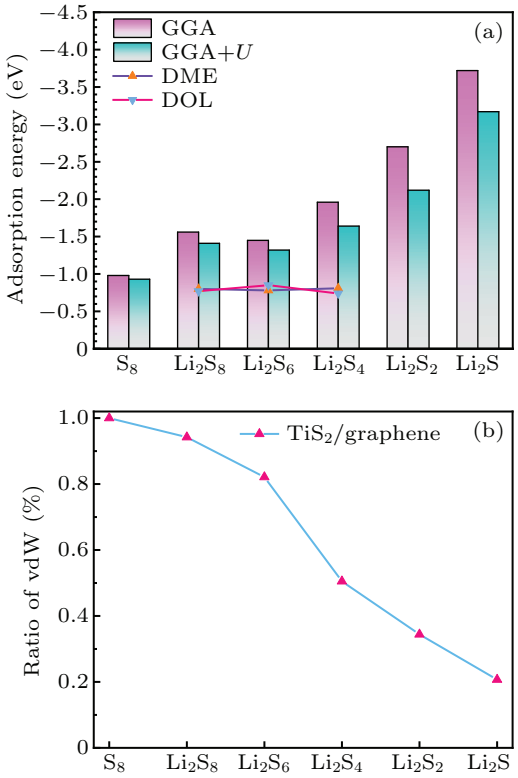



**Fig. 4.** (a) The adsorption energies of polysulfides with $TiS_2$/graphene heterostructure and their respective binding energies with two solvent molecules (DME and DOL) based on the GGA and the GGA+$U$ methods. (b) The proportion of van der Waals forces in a polysulfide-$TiS_2$/graphene heterostructure adsorption system.

To better understand the anchoring mechanism of the substrate material for lithium polysulfides, we calculated the proportion of vdW force in the adsorption energy ($R$), which is defined as

$$R = \frac{E_{ads}^{vdW} - E_{ads}^{novdW}}{E_{ads}^{vdW}} \times 100\%, \tag{3}$$

where $E_{ads}^{vdW}$ and $E_{ads}^{novdW}$ indicate the adsorption energies calculated with and without the vdW interactions, respectively. As shown in Fig. 4(b), the vdW force plays a very important role in the non-lithization stage. When $S_8$ molecules are adsorbed on the surface of the heterostructure, the $R$ is close to

100%, which is almost pure physical adsorption. With the lithization process, the proportion of vdW force physical interaction in the adsorption system decreases gradually. The proportion of vdW force in the adsorption system of long-chain lithium polysulfides ($Li_2S_n$, $n = 4$, 6, 8) is between 51% and 94%, which indicates that vdW force has an important contribution to the adsorption energy of long-chain lithium polysulfides. While the $R$ values of short-chain $Li_2S$ and $Li_2S_2$ adsorbed on the surface of the heterostructure are 21% and 34%, respectively, indicating that the adsorption between short-chain lithium polysulfides and the heterostructure is mainly based on chemical interaction. Hence, in the simulation process of the lithium-sulfur batteries, the correction of van der Waals's long-range interaction must be considered. Moreover, its huge vdW force ratio for long-chain lithium polysulfides shows that it is very difficult to anchor lithium polysulfide to the cathode because the vdW force is much weaker than chemical bonding.

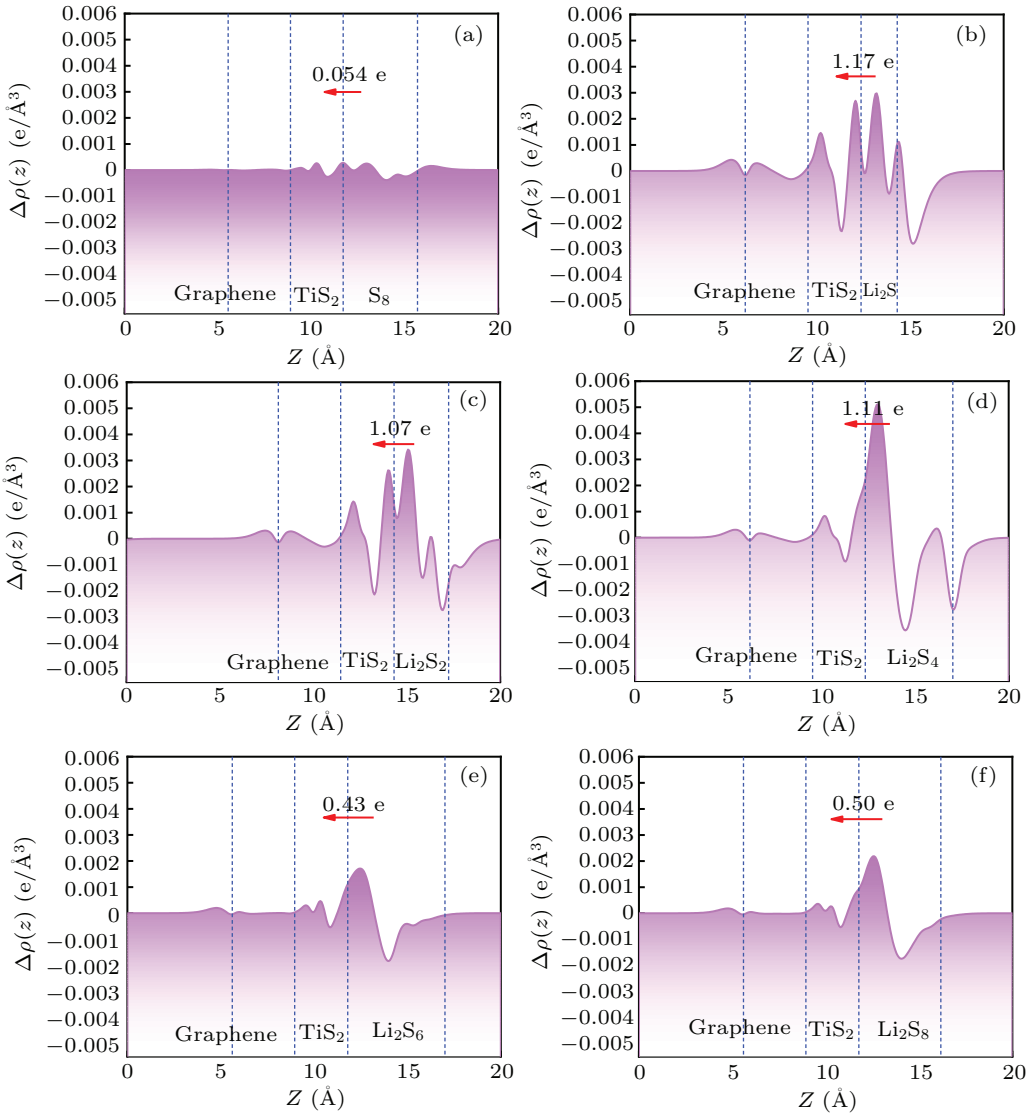



**Fig. 5.** Planar average charge density difference (purple lines) along the $z$-direction between polysulfide molecules and $TiS_2$/graphene heterostructure. The polysulfide molecules include (a) $S_8$, (b) $Li_2S$, (c) $Li_2S_2$, (d) $Li_2S_4$, (e) $Li_2S_6$, (f) $Li_2S_8$.

After discussing the adsorption system of polysulfides and heterostructure, the $z$-direction PCDD of polysulfides-adsorbed heterostructure was calculated to investigate the interaction between polysulfides and heterostructure, as shown in Figs. 5(a)–5(f). When polysulfide molecules are adsorbed on the surface of the heterostructure, there was almost no charge transfer for the graphene. The main charge transfer occurs between $TiS_2$ monolayer and polysulfide molecules, which is related to the newly formed covalent bond between Li and surface sulfur at the interface. There is almost no charge transfer between the non-lithium $S_8$ molecule and the substrate, which is directly related to the physical adsorption between them. For the adsorption system with long-chain lithium polysulfides $Li_2S_n$ ($n = 6$, 8), the charge is transferred from the Li atoms of the $Li_2S_n$ molecule to the surface S atoms of $TiS_2$ monolayer, and the new Li–S bonds are formed at the interface. For the adsorption system with short-chain lithium polysulfides $Li_2S_n$ ($n = 1$, 2, 4), the charge is trans-

ferred from the $Li_2S_n$ molecules to the $TiS_2$ monolayer in a relatively complicated way. Both sulfur and lithium atoms in the $Li_2S_n$ molecules provide the transferred electrons, which is mainly related to the small sulfur coordination number of lithium in the $Li_2S_n$ molecule. In addition, we quantitatively calculated the amount of charge transfer between $S_8$/$Li_2S_n$ and the substrate through Bader charge analysis. The charge transfer between $S_8$ molecules and the substrate is almost zero, which is also consistent with the analysis results of PCDD. However, the amount of charge transferred from $Li_2S_n$ ($n = 1$, 2, 4, 6, 8) to the substrate ranges from 0.50 to 1.17. It can be found that charge transfer is mainly used to form new Li-S covalent bonds at the interface. These bonds play a vital role in the anchoring of polysulfide molecules, and the amount of charge transfer has the same law as the adsorption energy, which further clarifies the internal adsorption mechanism associated with it.

The sulfur, as the cathode material of lithium-sulfur batteries, has poor electrical conductivity, the electronic conductivity of the added anchoring materials should be excellent to improve the weak conductivity of sulfur. The above calculations show that the $TiS_2$/graphene heterostructure has significant metallicity, and the electronic structure near the Fermi level of graphene is preserved. Therefore, graphene will provide very excellent electronic conductivity. To further illustrate the electronic conductivity of the anchoring material after the adsorption of lithium polysulfides, the total electron density of state (TDOS) and the projected density of state (PDOS) of $TiS_2$/graphene heterostructure adsorbed polysulfides were calculated. As shown in Fig. 6, the Fermi level of $TiS_2$/graphene heterostructure after adsorption of polysulfides has shifted. The abundant electronic states at the Fermi level indicate that the adsorption system still maintains good metallic properties, which greatly improves the poor electrical conductivity of the sulfur-based cathode material. Atom-projected state analysis shows that the states near the Fermi level are mainly derived from the contribution of the $TiS_2$ monolayer. Although the contribution of graphene seems relatively small from the results of PDOS, its excellent electronic conductivity will play an important role in improving the overall electronic conductivity of the cathode. As shown in Fig. 6(g), there is a potential barrier between graphene and the $TiS_2$ monolayer, which hinders the transfer of electrons between graphene and the polysulfides.[38] However, due to the existence of tunneling electrons, both graphene and the $TiS_2$ monolayer can be used as conductive channels for electron transport, and the overall conductivity of the heterostructure is stronger than that of pure $TiS_2$. Moreover, weaker adsorption dominated by vdW forces corresponds to high tunneling barriers, such as $S_8$, $Li_2S_8$, and $Li_2S_6$. While strong adsorption dominated by strong covalent bonds corresponds to low or no barriers, such as $Li_2S_n$ ($n = 1$, 2, 4). This strongly suggests that enhancing the interaction between polysulfide molecules and the substrate is not only beneficial for weakening the shuttle effect but can also reduce the internal resistance of the electrode.

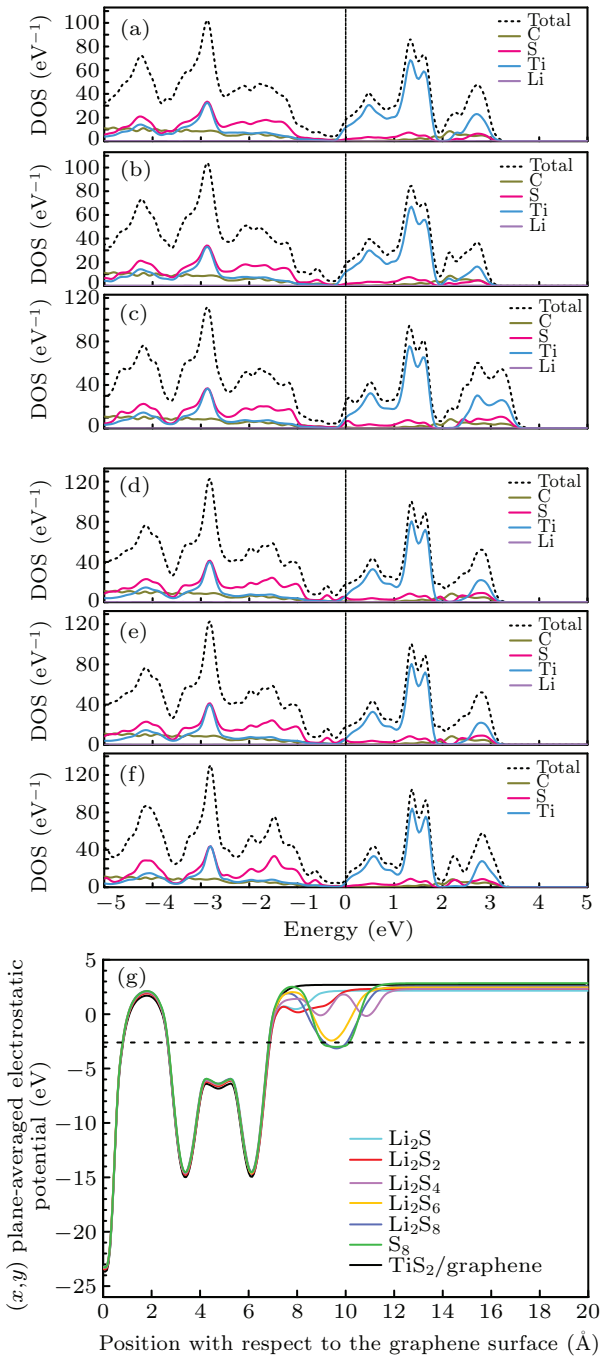



**Fig. 6.** Density of states (DOS) of (a) $S_8$, (b) $Li_2S$, (c) $Li_2S_2$, (d) $Li_2S_4$, (e) $Li_2S_6$, (f) $Li_2S_8$ adsorbed on $TiS_2$/graphene heterostructure. (g) The plane-averaged electrostatic potential above the graphene for adsorption of $S_8$ and $Li_2S_n$ ($n = 1$, 2, 4, 6, 8).

The diffusion performance of Li-ion on the surface of heterostructure is another important criterion for evaluating heterostructure as the anchoring material of lithium-sulfur batteries, which will significantly affect the charge-discharge performance of the cell. The charge–discharge process of lithium-sulfur batteries can be simplified as $Li_2S \rightarrow LiS + Li^+ + e^-$,

that is the decomposition process of $Li_2S$ and the migration process of Li-ion. The CI-NEB method was used to simulate these two processes and the corresponding potential barriers. As shown in Fig. 7, the path from site-1 to site-2 simulates the decomposition process of $Li_2S$. This process is accompanied by the breaking of the Li–S bond in $Li_2S$. The decomposition potential barrier of $Li_2S$ is 0.28 eV. Compared to some other two-dimensional materials like FeS ($\sim$ 0.63 eV),[39] graphene ($\sim$ 1.8 eV),[39] $V_2CS_2$ (0.53 eV),[40] $V_2CO_2$ (0.43 eV),[40] blue phosphorene (0.55 eV and 0.50 eV),[41] and $CoS_2$ ($\sim$ 0.56 eV),[39] the $TiS_2$/graphene heterostructure exhibits advantageous performance. Such a small value indicates that the heterostructure can effectively catalyze the decomposition of $Li_2S$. The path from site-2 to site-3 simulates the process of Li-ions getting rid of the influence of the lithium polysulfide group. The migration barrier of this process is 0.22 eV, slightly lower than the decomposition barrier of $Li_2S$, indicating that Li-ions can easily escape from the lithium polysulfide group. The path from site-3 to site-4 mimics the process of free migration of Li-ions on the surface of the heterostructure after getting rid of the influence of the lithium polysulfide group. The calculated results show that the migration barrier of this process is equal to that of the process from sites-2 to site-3, both of which are 0.22 eV. This value is close to that of other two-dimensional materials such as $V_2CO_2$ (0.26 eV),[40] $V_2C$ (0.19 eV),[40] $Ti_3CNO_2$ (0.26 eV),[42] $MoSe_2$ (0.24 eV),[43] and $Ti_2NS_2$ ($\sim$ 0.19 eV).[44] Such a low migration barrier can greatly promote the conversion of lithium polysulfides to $S_8$ molecules.

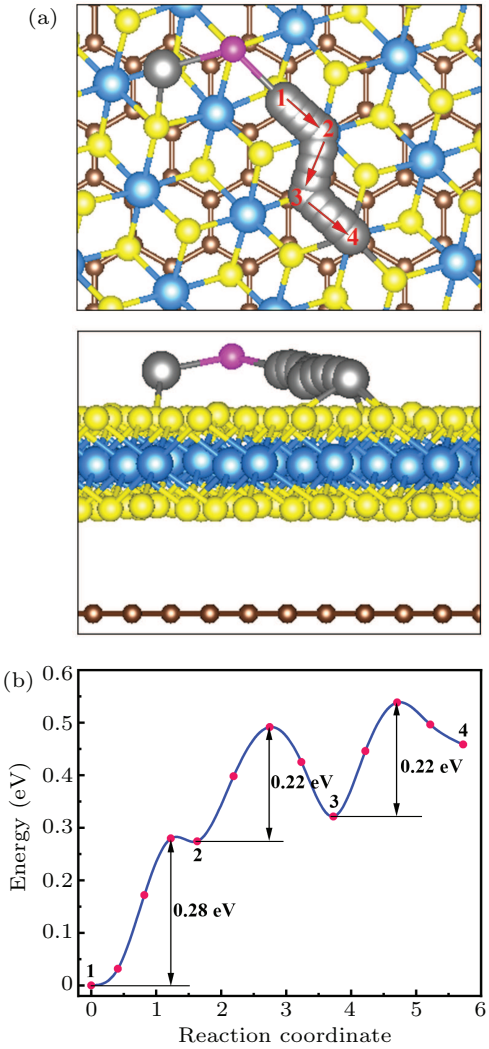



**Fig. 7.** (a) The path and (b) potential energy curve of $Li_2S$ dissociation on $TiS_2$/graphene heterostructure.

## 4. Conclusion and perspectives

In this paper, we comprehensively analyze the potential of $TiS_2$/graphene heterostructure as an anchoring material for lithium-sulfur batteries through first-principles calculations. The electronic structure calculations show that the $TiS_2$/graphene heterostructure has intrinsic metallicity, and the formation of the heterostructure does not significantly change the electronic properties of the two monolayer materials. The excellent electrical properties of graphene can be used to improve the weak conductivity of the sulfur cathode, and the polarity of $TiS_2$ monolayer can be used to enhance the anchoring effect of lithium polysulfides. The charge transfer diagram of the heterostructure shows that the formation of the heterostructure leads to the charge transfer from graphene to the $TiS_2$ monolayer, which further enhances the polarity of the heterostructure and promotes the anchoring of polysulfides. The adsorption simulations of polysulfide molecules and heterostructures show that the adsorption energy higher than 1.5 eV endows the heterostructure with strong anchoring ability. The analysis of the adsorption energy components shows that the high proportion of vdW force may be an important reason why lithium polysulfides are uneasy to anchor. Further charge transfer analysis also shows that there is a corresponding relationship between the strength of adsorption and the amount of charge transfer. The calculation of the electronic structure of the adsorption system shows that the heterostructure system can still maintain metallicity after adsorption, and graphene can also exert its excellent electronic conductivity. The simulation of $Li_2S$ dissociation on the surface of the heterostructure shows that the heterostructure can well catalyze the dissociation of polysulfides, and the dissociated Li-ions can migrate freely on the surface. Therefore, the $TiS_2$/graphene heterostructure will be an ideal anchoring material for lithium-sulfur batteries. We hope that our work will encourage more experimental or theoretical research to further explore the potential of other novel 2D heterostructures as anchoring materials for lithium-sulfur batteries.

## Acknowledgements

Project supported by the National Natural Science Foundation of China (Grant Nos. 62104168, 11604235, and

U1510132), the Beijing Institute of Technology Research Fund Program for Young Scholars, the Natural Scientific and Technological Innovation Programs of Higher Education Institutions in Shanxi, China (Grant No. 2019L0309), the Natural Science Foundation of Shanxi Province, China (Grant Nos. 201901D111125 and 20210302123201), and the Shanxi Scholarship Council of China.

## References

[1] Etacheri V, Marom R, Elazari R, Salitra G and Aurbach D 2011 *Energ. Environ. Sci.* **4** 3243
[2] Goodenough J B and Kim Y 2010 *Chem. Mater.* **22** 587
[3] Wei Z, Tseng K J, Wai N, Lim T M and Skyllas-Kazacos M 2016 *J.Power Sources* **332** 389
[4] Li Y, Feng Y, Sun X and He Y 2017 *Angew. Chem. Int. Ed.* **56** 5734
[5] Yang Y, Zheng G and Cui Y 2013 *Chem. Soc. Rev.* **42** 3018
[6] Manthiram A, Fu Y, Chung S H, Zu C and Su Y S 2014 *Chem. Rev.* **114** 11751
[7] Chen X, Hou T, Persson K A and Zhang Q 2019 *Mater. Today* **22** 142
[8] Chung W J, Griebel J J, Kim E T, Yoon H, Simmonds A G, Ji H J, Dirlam P T, Glass R S, Wie J J, Nguyen N A, Guralnick B W, Park J, Somogyi A, Theato P, Mackay M E, Sung Y E, Char K and Pyun J 2013 *Nat. Chem.* **5** 518
[9] Lu S, Cheng Y, Wu X and Liu J 2013 *Nano Lett.* **13** 2485
[10] Zhao M Q, Zhang Q, Huang J Q, Tian G L, Nie J Q, Peng H J and Wei F 2014 *Nat. Comm.* **5** 3410
[11] Zhou G, Li L, Wang D W, Shan X Y, Pei S, Li F and Cheng H M 2015 *Adv. Mater.* **27** 641
[12] Dong Y, Zheng S, Qin J, Zhao X, Shi H, Wang X, Chen J and Wu Z S 2018 *Acs Nano* **12** 2381
[13] Liang X, Rangom Y, Kwok C Y, Pang Q and Nazar L F 2017 *Adv. Mater.* **29** 1603040
[14] Majumder S, Shao M, Deng Y and Chen G 2019 *J. Power Sources* **431** 93
[15] Wang H, Yang Y, Liang Y, Robinson J T, Li Y, Jackson A, Cui Y and Dai H 2011 *Nano Lett.* **11** 2644
[16] Zhou G, Pei S, Li L, Wang D W, Wang S, Huang K, Yin L C, Li F and Cheng H M 2014 *Adv. Mater.* **26** 625
[17] Qiu Y, Li W, Zhao W, Li G, Hou Y, Liu M, Zhou L, Ye F, Li H, Wei Z, Yang S, Duan W, Ye Y, Guo J and Zhang Y 2014 *Nano Lett.* **14** 4821
[18] Huang J Q, Zhuang T Z, Zhang Q, Peng H J, Chen C M and Wei F 2015 *Acs Nano* **9** 3002
[19] Zhu X, Zhao W, Song Y, Li Q, Ding F, Sun J, Zhang L and Liu Z 2018 *Adv. Energ. Mater.* **8** 1800201
[20] He J, Hartmann G, Lee M, Hwang G S, Chen Y and Manthiram A 2019 *Energ. Environ. Sci.* **12** 344
[21] Kresse and Furthmuller 1996 *Phys. Rev. B* **54** 11169
[22] Mezei P D, Csonka G I and Kallay M 2017 *J. Chem. Theor. Comput.* **13** 4753
[23] Blochl 1994 *Phys. Rev. B* **50** 17953
[24] Grimme S, Ehrlich S and Goerigk L 2011 *J.Comput. Chem.* **32** 1456
[25] Grimme S, Antony J, Ehrlich S and Krieg H 2010 *J. Chem. Phys.* **132** 154104
[26] Henkelman G, Uberuaga B P and Jonsson H 2000 *J. Chem. Phys.* **113** 9901
[27] Henkelman G and Jonsson H 2000 *J. Chem. Phys.* **113** 9978
[28] Wang B, Alhassan S M and Pantelides S T 2014 *Phys. Rev. Appl.* **2** 034004
[29] Jiang H R, Shyy W, Zeng L, Zhang R H and Zhao T S 2018 *J. Mater. Chem. A* **6** 13244
[30] Kosa M and Major D T 2015 *Crystengcomm* **17** 295
[31] Li Y, Wu W and Ma F 2019 *J. Mater. Chem. A* **7** 611
[32] Su J, Li W, Duan T, Xiao B, Wang X, Pei Y and Zeng X C 2019 *Carbon* **153** 767
[33] Zhang W X, Yin Y and He C 2020 *Phys. Chem. Chem. Phys.* **22** 26231
[34] Zhang W X, Yin Y and He C 2021 *J. Phys. Chem. Lett.* **12** 5064
[35] Zhang T, Wang H and Zhao J 2019 *New J. Chem.* **43** 9396
[36] Zhao Y and Zhao J 2017 *Appl. Surface Sci.* **412** 591
[37] Wang L, Zhang T, Yang S, Cheng F, Liang J and Chen J 2013 *J. Energ. Chem.* **22** 72
[38] Li S, Mou T, Ren G, Warzywoda J, Wang B and Fan Z 2016 *Acs Energ. Lett.* **1** 481
[39] Zhou G, Tian H, Jin Y, Tao X, Liu B, Zhang R, Seh Z W, Zhuo D, Liu Y, Sun J, Zhao J, Zu C, Wu D S, Zhang Q and Cui Y 2017 *Proc. Natl. Acad. Sci. USA* **114** 840
[40] Wang Y, Shen J, Xu L C, Yang Z, Li R, Liu R and Li X 2019 *Phys. Chem. Chem. Phys.* **21** 18559
[41] Mukherjee S, Kavalsky L, Chattopadhyay K and Singh C V 2018 *Nanoscale* **10** 21335
[42] Chen X, Kong Z, Li N, Zhao X and Sun C 2016 *Phys. Chem. Chem. Phys.* **18** 32937
[43] Wong H, Ou X, Zhuang M, Liu Z, Hossain M D, Cai Y, Liu H, Lee H, Wang C Z and Luo Z 2019 *Acs. Appl. Mater. Interfaces* **11** 19986
[44] Shukla V, Jena N K, Naqvi S R, Luo W and Ahuja R 2019 *Nano Energy* **58** 877